

Bachelor Research Project

Targeting TNF- α Receptor Signaling in Alzheimer's Disease: Effects on Synaptic Plasticity, Oligodendrocytes, and Working Memory

Author: Léon Spa (S5220548)

Supervisors: Giulia Mozzanica, Jiahao Li, Wanda Douwenga & Ulrich L. M. Eisel

Faculty of Science and Engineering

program: (BSc) Biology , Neuroscience and behaviour

date: 28-05-2025

Abstract:

Alzheimer's disease (AD) is characterized by the accumulation of amyloid- β plaques, tau neurofibrillary tangles and chronic inflammation, all of which contribute to cognitive decline. Tumor necrosis factor-alpha (TNF- α) has emerged as a key player in this inflammatory process and acts through two receptors: TNF receptor 1 (TNFR1), which promotes inflammation and cell death, and TNF receptor 2 (TNFR2) which is known to be involved in neuroprotection. This study assessed whether modulating TNF signaling could serve as a viable therapeutic strategy. Immunohistochemistry targeting neuronal density (NeuN), Synaptic plasticity (Synapsin-1) and oligodendrocyte density (Olig2) was performed on wild-type, J20, and triple transgenic (3xTg) mouse brain slices. Additionally, we evaluated STAR2's (a TNFR2 agonist) potential as a drug using MTT assays on Kym-1 cells. Finally, we analyzed short-term working memory in a behavioral analysis on J20 mice using a Y-maze after a TNFR1 antagonist treatment. The immunostainings did not yield many usable results due to a poor signal and/or high background noise. However, the cytotoxicity assay revealed a clear negative correlation between STAR2 concentration and Kym-1 cell viability, especially for STAR2 stored at 37°C however, this effect was possibly partially explained due to toxic degradation products. The Y-maze results revealed no significant behavioral improvements, likely due to short-term memory being rescued by the prefrontal cortex and ventral striatum. The results suggest that while TNF signaling modulation holds potential, future studies should refine both experimental design and behavioral assays to better evaluate cognitive outcomes.

Introduction:

As people continue to get older, neurodegenerative diseases (ND's) are becoming an increasingly pressing concern. The most common ND in the world is Alzheimer's disease contributing to 60-70% of dementia cases worldwide (World Health Organization: WHO & World Health Organization: WHO, 2025). In Alzheimer's disease amyloid β plaques, tau neurofibrillary tangles, and chronic inflammation are known to cause many of the phenotypical changes of the disease. Unfortunately, current treatment options leave a lot to be desired since they are primarily anti-symptomatic and don't tackle the cause of the disease or are simply just not effective enough (Zhang et al., 2024). While every ND has its own defining features, protein aggregation and chronic inflammation are two common pathological mechanisms (Wilson et al., 2023). Inflammation, in particular, is known to cause excessive neuronal cell death and has thus emerged as a promising therapeutic target (Ortí-Casañ et al., 2019) (Ortí-Casañ et al., 2022).

One of the central players within this inflammatory response is called tumor necrosis factor α (TNF- α) (Dong et al., 2015). TNF- α is primarily produced by monocytes and macrophages and is present in two forms, being in its soluble form (sTNF) and its membrane-bound form (mTNF) (Skartsis et al., 2022). sTNF can bind to TNFR1 and mTNF can bind both to TNFR1 and TNFR2. Even though both receptors share NF- κ B as one of their main end products in their intracellular pathways, they contribute to a very opposing effect in the brain (Fontaine et al., 2002) (Decourt et al., 2016). TNFR1 activation has been shown to promote inflammation and cell death by acting through sensitizing pro-inflammatory molecules like lipocalin-2 (Naudé et al., 2012), while downstream molecules of the TNFR2 receptor are known to be involved in neuroprotection. For example, through improving neuronal resistance against excitotoxicity (Marchetti et al., 2004) or through improving microglial phagocytosis of A β plaques (Ortí-Casañ et al., 2023). Microglia, the resident immune cells of the central nervous system, play a key role in maintaining brain homeostasis and responding to injury or disease (Prinz et al., 2019). Studies have shown that when microglia get stressed, they shift to a pro-inflammatory phenotype, secreting more cytokines like TNF- α , this shift can cause a downward spiral, further progressing the disease (Fischer et al., 2015) (Ortí-Casañ et al., 2023). Another effect of a pathological TNF homeostasis is that synaptic plasticity gets impaired in AD brains (Dong et al., 2015), serving as a marker for the disease. Furthermore oligodendrocyte regeneration is stimulated through TNFR2 activation (Dong et al., 2016) whilst TNFR1 promotes oligodendrocyte death (Steelman & Li, 2011) implying that the imbalanced TNF homeostasis in AD patients is likely to affect oligodendrocyte density. Global inhibition of TNF signaling through for example, etanercept, a drug that inhibits TNF- α , has been shown to be effective (Fischer et al., 2015). Nevertheless, the direct inhibition of TNF- α showed detrimental effects due to TNF- α 's crucial role in the immune system (Dong et al., 2016) (Fischer et al., 2015). A way to prevent these detrimental effects would be to selectively block only the TNFR1 signaling or increase TNFR2 signaling by introducing an agonist for this receptor. Several papers investigate the approach of introducing a TNFR2 agonist, and in these studies a drastic reduction of amyloid β deposition and β -secretase 1 expression was observed (Dong et al., 2016) (Ortí-Casañ et al., 2022). The β -secretase 1 gene is responsible for cleaving the amyloid precursor protein into the amyloid- β peptides responsible for the plaque pathologies (Hampel et al., 2020). To check for the effectiveness of the STAR2 compound, we look at its interaction with the Kym-1 cell line. These cells are known to express both TNFR1 & TNFR2 and are known to die upon strong interactions with the TNFR2 receptors. Thus, cell viability can be used to assess a TNFR2 agonist's effectiveness (Bourteele et al., 1998) (Storz et al., 2000) (Jupp et al., 2001).

During our studies the J20 mouse model was used to mimic AD pathology. This transgenic model has been made such that it overexpresses the amyloid precursor protein (APP) with familial AD mutations (Tosh et al., 2018). During the immunohistochemical stainings, not only did we use WT and J20 mouse brain slices but also 3xTg brain slices. In this model also the tau neurofibrillary tangles are present so they can be taken into the equation when comparing brain slices.

In this report, we will use Neun, Synapsin-1 and Olig 2 staining to assess neuronal density, synaptic plasticity and oligodendrocyte density to assess the state of the disease in wild-type, J20 and 3xTg mouse brain tissue. But most importantly, we will investigate the effects of modulating TNF homeostasis to assess its viability in Alzheimer's disease treatment to answer the question: Is TNF(- α) modulation a viable therapeutic approach to improve working memory in murine Alzheimer's disease models?? To do this, we will assess 3 immunohistochemical stainings, Kym cell viability after treatment at different concentrations of STAR 2 stored at either 4°C or 37°C and analyze Y-maze behavioral videos to test short-term working memory in J20 mice.

Methods:

2.1 Mice models

Mice samples for the immunohistochemical stainings and Y-maze videos were procured by the University of Groningen. For staining, we employed J20 and triple transgenic (3xTg) mice. J20 mice are genetically modified to overexpress the human amyloid precursor protein (via the expression of Swedish and Indiana mutations), resulting in recognizable AD characteristics, including amyloid plaque buildup, loss of synapses and neurons, and behavioral deficits (Karl et al., 2012; Hong et al., 2016; Tosh et al., 2018). Alternatively, 3xTg mice develop both amyloid plaque and neurofibrillary tangles in AD related brain areas (via the expression of PS1M146V, APPSWE, and tauP301L mutations), also leading to cognitive deficits and reduction in synaptic plasticity (Oddo et al., 2003). For the control slices we used Groningen wild-type mice. Mice had access to food and water ad libitum and were on a 12:12 light/dark cycle. For the Y-maze experiments both male and female J20 mice were used. The behavioural tests were always performed during the light phase of the cycle. All experiments were approved by the animal ethics committee of the University of Groningen

Immunohistochemical Staining for Olig2

Coronal brain slices were stored in a cryoprotectant solution and transferred to TBS 0.01M and were washed three times for 5min with clean TBS 0.01M pH 7.4 followed by 1h of pre-incubation in blocking buffer (3% BSA + 0.3% Triton-X in 0.001M TBS pH 7.4). Primary antibody incubation was done overnight at 4°C on shaker (1:500 rabbit anti-Olig2, 3% BSA , 0.3% Triton-X in 0.001M TBS pH 7.4). Next, the samples were washed six times for 5 mins with TBS 0.01M pH 7.4. Working in the dark, secondary antibody incubation was done (1:400 donkey anti-rabbit-Alexa Fluor 488, 3% BSA, 0.3% Triton-X in 0.001M TBS pH 7.4) for 2 hours at room-temperature. Samples were again rinsed three times for 5 mins with TBS 0.01M pH 7.4, and incubated overnight at 4°C on shaker. Samples were mounted with Vectashield antifade mounting medium, then a coverslip was added.

Immunohistochemical Staining for NeuN

Coronal brain slices were stored in a cryoprotectant solution and transferred to TBS 0.01M and were washed three times for 5min with clean TBS 0.01M pH 7.4 followed by 1h of pre-incubation in blocking buffer (5% BSA, 0.5% Triton-X in 0.001M TBS pH 7.4). Primary

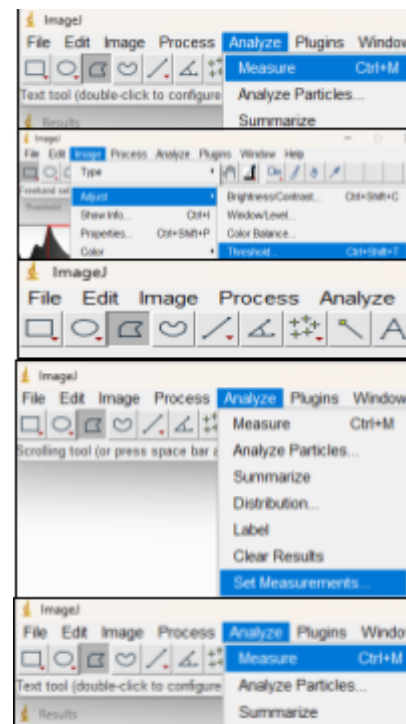
antibody incubation was done overnight at 4°C on shaker (1:500 mouse anti-NeuN, 5% BSA, 0.5% Triton-X in 0.001M TBS pH 7.4). Next, the samples were washed six times for 5 mins with TBS 0.01M pH 7.4. Working in the dark, secondary antibody incubation was done (1:400 anti-rabbit Alexa Fluor 488, 5% BSA, 0.5% Triton-X in 0.001M TBS pH 7.4) for 2 hours at room temperature. Samples were again rinsed six times for 5 mins with TBS 0.01M pH 7.4, and incubated overnight at 4°C on shaker. Samples were mounted with Vectashield antifade mounting medium, then a coverslip was added.

Immunohistochemical Staining for Synapsin-1

Coronal brain slices were stored in a cryoprotectant solution and transferred to TBS 0.01M and were washed three times for 5min with clean TBS 0.01M pH 7.4 followed by 1h of pre-incubation in blocking buffer (5% Normal Donkey Serum (NDS), 0.5% Triton-X in 0.001M TBS pH 7.4.) Primary antibody incubation was done overnight at 4°C on shaker (1:500 mouse anti-Synapsin-1, 3% BSA , 0.5% Triton-X in 0.001M TBS pH 7.4). Next, the samples were washed six times for 5 mins with TBS 0.01M pH 7.4. Working in the dark, secondary antibody incubation was done (1:400 anti-rabbit Alexa Fluor 488, 1% NDS, 0.3% Triton-X in 0.001M TBS pH 7.4) for 2 hours at room temperature. Samples were again rinsed six times for 5 mins with TBS 0.01M pH 7.4, and incubated overnight at 4°C on shaker. Samples were mounted with Vectashield antifade mounting medium, then a coverslip was added.

Image analysis

Staining images were taken using a Leica DMi6000 Inverted Fluorescence Microscope at either a 10x or 20x magnification. The staining results were subsequently quantified using ImageJ software by measuring the Area % of coverage within the region of interest, specifically the hippocampus. This is achieved by making sure the image is in 16 bit. Threshold was adjusted so that as little background signal was present and as much signal of interest was isolated. These threshold settings were applied to all images of the same stain. With the polygon tool the area of interest was selected. Through analyze, set measurements Area fraction was selected. after clicking the image Ctrl + M was used to obtain the area percent signal. The percentage area of signal was then graphically represented using R-studio.



Cytotoxicity Assay on Kym-1 cells

To test for the stability of the STAR2 a cytotoxicity assay was performed using an MTT assay in Kym-1 cells. STAR2 was placed in an incubator for more than a year at 37°C and its bioactivity was compared with that of STAR2 stored at 4°C. The Kym-1 cells were cultivated in RPMI medium supplemented with 1% penicillin streptomycin + 1% l-glutamine + 10% Fetal Bovine Serum (CO₂ incubator, 5%-10% CO₂).

The Kym-1 cells (1.5x10⁴ cells/well) were transferred to 96-well cell-culture plates and treated with 10, 100, or 1000 ng/ml of STAR2 stored at 4°C or 37°C. A total of 24 wells served as controls, with 6 wells allocated to each treatment condition. Cells were washed with PBS, then PBS

with 5mg/ml MTT solution was added to each well followed by 2 hours of incubation (CO₂ incubator, 5%-10% CO₂). After discarding the supernatant, cells were stored at -80°C overnight. The following day, the plates were incubated at 37 °C for 30 minutes, after which 150 µl of DMSO was added. The next day, the plates were incubated at 37 °C for 30 minutes, followed by the addition of 150 µl of DMSO. Absorbance was then recorded at 570 nm using a spectrophotometer.

Genotyping

For DNA isolation a commercially available NucleoSpin tissue kit was used. Mouse tail snips were treated with 180 µL of buffer T1 and 25 µL of proteinase K, then incubated overnight at 56°C to be digested. Samples were centrifuged at 11,000 × g for 5 minutes to pellet remaining hair and bone fragments. The supernatant was transferred to a new tube containing 200 µL of buffer B3 and 210 µL of 100% ethanol. After vortexing, the mixture was incubated at 70°C for 10 minutes. DNA isolation was performed using spin columns: 500 µL of buffer BW and 600 µL of buffer B5 were added sequentially, each followed by centrifugation at 11,000 × g for 1 minute. After a dry spin, DNA was eluted with a preheated (70°C) elution buffer and collected by final centrifugation.

For PCR amplification, the master mix (per 20 µL reaction) contained 14.92 µL nuclease-free water, 2 µL DreamTaq buffer, 0.4 µL 10 mM dNTPs, 0.4 µL each of forward and reverse primers at 10 µM (see Table 1), 0.08 µL DreamTaq DNA polymerase, and 1 µL genomic DNA. PCR cycling conditions were: initial denaturation at 94°C for 2 minutes; 33 cycles of 94°C for 30 seconds (denaturation), 60°C for 30 seconds (annealing), and 72°C for 1 minute (extension); followed by a final extension at 72°C for 7 minutes. PCR products were separated on a 1% agarose gel run at 80 mA for 1 hour and visualized using a Chemidoc system.

Table 1
Primers used for PCR

Identifier	Genotype	Primer	Sequence (5'-3')
IMR8744	J20-negative	Forward	CAAATGTTGCTTGTCTGGTG
IMR8745	J20-negative	Reverse	GTCAGTGTCACAGTTTG
IMR2044	J20 Transgene	Forward	GTGGAGTTTGTAAGTGATGCC
IMR2045	J20 Transgene	Reverse	TCTTCTTCTCAACCTCAGC

Y-maze

To evaluate working memory in J20 mice treated with either PBS or the TNFR-1 antagonist, Y-maze videos were analyzed. All of the Y-maze arms (A, B & C) were empty and readily accessible. In total, 23 treatment & genotype blinded videos were examined. For ten minutes, each mouse was scored based on the sequence of arms it entered. An entry was confirmed when the mouse placed all four legs into the arm. With this, percentage alternation was calculated based on triads and total arm visits. A triad consists of a sequence of 3 different arm entries so ABC and CAB are triads, and BCB is not. To calculate the percentage alternation the following formula is used: number of triads/(total entries-2) x 100% = percentage alternation.

Statistical analysis

To analyse the data, several statistical tests were performed in R-studio. For the MTT assay results, normality of the data was assessed using the Shapiro-Wilk test, and homogeneity of variances was checked with Levene's test. Based on these results, the personal results were analyzed using a

two-way ANOVA ($p < 0.05$) paired with a Tukey's multiple comparisons post-hoc test to see which groups hold a significant difference over each other. Given the non-parametric distribution of the grouped data, a two-way Aligned Rank Transform ANOVA (ART-ANOVA) was performed, combined with a Tukey's multiple comparisons post-hoc test. Finally, a Pearson's R correlation test was performed to see if a linear relation was present between the concentration and cell viability. Another two-way ANOVA was performed on the Y-maze video results to compare groups. Statistical significance was accepted at $p < 0.05$. All data are presented as mean \pm standard error of the mean (SEM).

Results:

Staining of brain slices.

During our research, multiple biomarkers for AD pathologies were tested and visualized in Figure 1 below. Due to time constraints, only one slice per condition was analyzed in ImageJ, making statistical analysis infeasible. Each staining consisted of a DAPI stain to stain all nuclei in blue and each respective protein in green. For the Olig-2 stain (figure 1A) some signal was obtained, primarily visible in the triple transgenic slice (Figure 1 E-G). The red arrows indicate an area with a clearly visible Olig-2 signal and thus oligodendrocytes. For the other mouse models, there was no clear signal present and thus the signal area% (figure 1D) comparison yielded no useful results except that our negative control worked. For the Synapsin-1 staining (figure 1B) it was also hard to determine if a signal was present because the background noise was too bright to nicely quantify the result using ImageJ. The Synapsin-1 negative control was lost somewhere during washing thus a NeuN negative control was taken. When looking at the NeuN (figure 1C) staining, it is clear the primary antibodies did not bind the neurons since no overlap of DAPI & NeuN is visible and the background signal is also very high, which becomes even more clear when looking at the signal area % (figure 1D) of the negative control rendering the results unusable.

Cytotoxicity Assay on Kym-1 cells

The MTT-assay's group (figure 2A) depict a clear trend in which the higher the concentration of STAR2 the less cell viability. This trend becomes significant when comparing the bar of 37°C 10ng/mL with 37°C 1000 ng/ml (p -value = 0.0019). The Pearson's R correlation coefficient between cell viability and concentration of the 37°C compound is -0.255 (p -value = 0.00402) and that of the 4°C compound is -0.0459 (p -value = 0.610) meaning that for the group result, the negative correlation between concentration and cell viability is only significant when looking at the 37°C compound. The results from my 96-well plate (figure 2B) are more in line with expectations. Here the difference in viability between 4°C 1000ng/ml and the control without STAR2 shows a significance decrease in cell viability (p -value = 0.0245) an even greater significance appears when looking at the 37°C 1000ng/ml and the control (p -value = 0.0012) when comparing the 37°C 1000ng/ml with the 37°C 10ng/ml group (p -value = 0.0011) a similar decrease in cell viability is visible. This together with the graphs suggest a negative relation between the concentration of STAR2 and cell viability. This statement gets supported through the Pearson's R correlation coefficient values for the 37°C compound of -0.754 (p -value = 0.000304) and -0.692 (p -value = 0.00146) for the 4°C compound. When looking at the 96-well plate prepared in a parallel experiment (figure 2D) the only significant difference in cell viability between different concentrations of STAR2 is between the control and the 37°C 1000 ng/ml groups (p -value = 0.0051). Pearson's R correlation coefficient for the 37°C compound was -0.76 (p -value = 0.0003) and 0.374 (p -value = 0.16) for the 4°C compound. So also here a strong negative

correlation was observed between STAR2 concentration and cell viability for the 37°C compound. One of the reasons the results differ so much between both individual plates is due to bacterial contamination; the wells on the plate from the parallel experiment contained a lot more formazan visible in tiny dots spread across the well (figure 2E). When this is compared to the wells in the other individual plate (figure 2C) it becomes clear why the results differ so much. The contamination was mainly present in the wells for the control and the 4°C compound; this further supports the abnormalities seen in the corresponding plot (figure 2D).

Y-maze behavioral analysis.

The two-way ANOVA statistical analysis revealed that there was no significant difference in average alternation between the TNFR1-antagonist treated group and the PBS-treated control group. Even when sexes are separated; no significant difference was found. After analyzing the data from the Y-maze videos, genotyping of the animals occurred 6 mice were genotyped (supplementary figure 1).

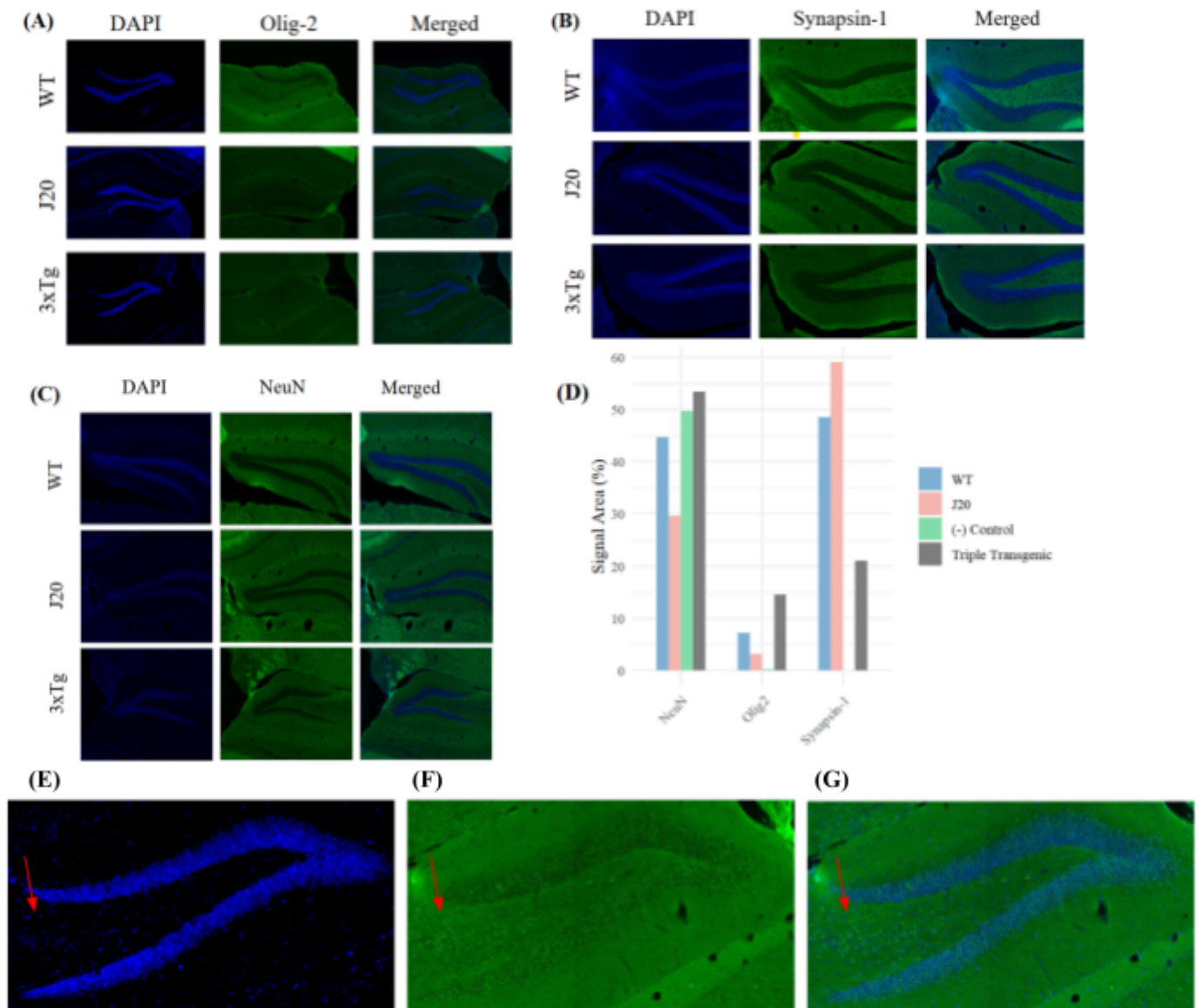


Figure 1: (A) Olig 2 staining results , (B) Synapsin-1 staining results, (C) NeuN staining results , (D)

Quantification of images through Singnal Area (%) using ImageJ software, (E) Zoomed-in DAPI staining of 3xTg Olig-2 brain slice, (F) zoomed in Olig-2 staining of 3xTg Olig-2 brain slice, (G) zoomed-in merged image of 3xTg Olig-2 brain slice.

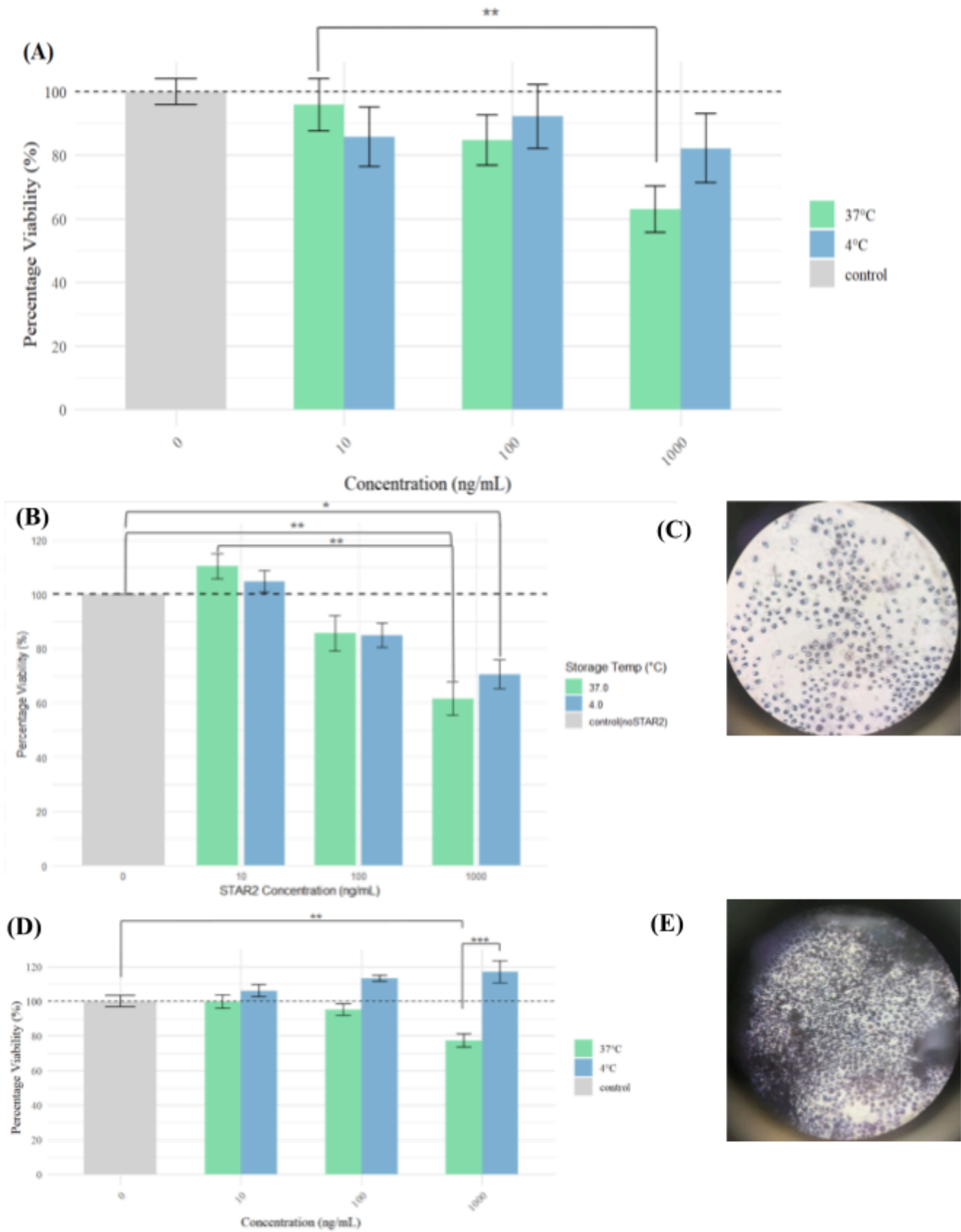


Figure 2: (A) Group results cytotoxicity MTT-assay Cell viability plotted against STAR2 concentration, (B) Own results cytotoxicity MTT-assay , (C) Clean well of Kym-1 cells under microscope (own plate), (D) parallel experiment results cytotoxicity MTT-assay , (E) Contaminated well of Kym-1 cells under microscope (parallel experiment), (for all statistical analysis (* = $p < 0.05$, ** = $p < 0.01$, *** $p < 0.001$))

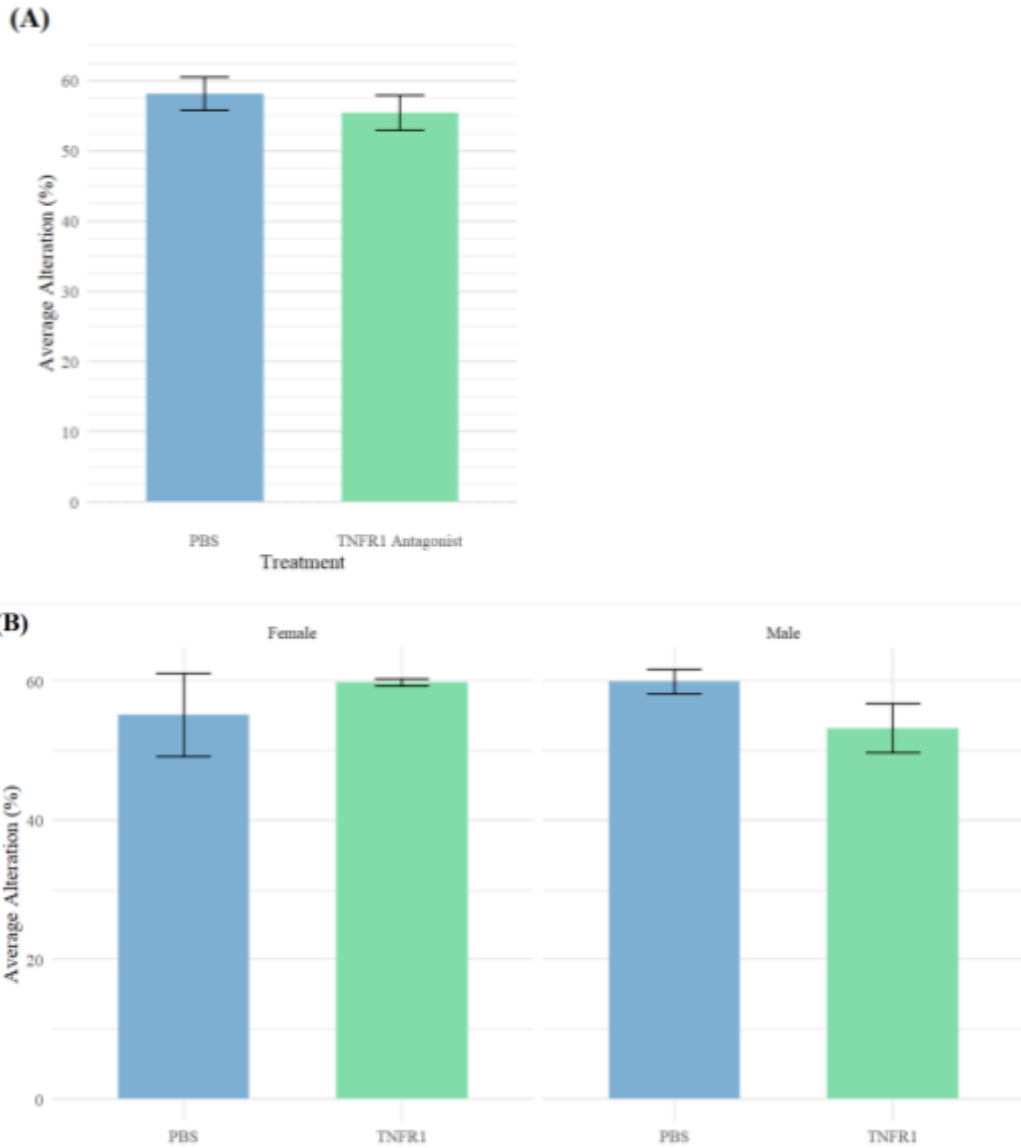


Figure 3: (A) Y-maze average alteration (total visits-2 / triads) per treatment, (B) Sex-separated Y-maze average alteration results (total visits-2 / triads) per treatment.

Conclusion & Discussion.

In this report, we aimed to answer the research question: Is TNF(- α) modulation a viable therapeutic approach to improve working memory in murine Alzheimer's disease models? To do this, we conducted several experiments consisting of 3 immunostainings, a cytotoxicity assay on Kym-1 cells and a Y-maze behavioral analysis. The immunostaining for Olig-2 & Synapsin yielded some antibody signal; however, due to high background noise and the inability to compare between the groups due to only some of the groups having a signal, this resulted in the inability to do a proper analysis. An extra point of discussion concerning the Synapsin-1 staining is that we lost the negative controls for this stain and were forced to use one of the NeuN negative controls for analysis. This did not show much unspecific binding after analysis in ImageJ. This, however, is pretty weird since for the NeuN staining, the negative control showed a lot of signal which could indicate high levels of unspecific binding or improper washing or blocking. So overall, the immunostaining results can not be considered useful and should be revised. Possible reasons could be improper washing of the slices or insufficient blocking in the case of unspecific binding. Another possibility is antibody degradation, as multiple lab groups reported similar staining issues. The addition of a positive control and extra careful washing and pipetting can be good ways to improve upon the previous attempt. Furthermore, trying another blocking agent can be a good way to reduce nonspecific binding sites (Ramos-Vara, 2005). It would also be of great interest to include TNFR1 antagonist or TNFR2 agonist treated mouse slides to see if the compounds can rescue any created damage.

For the cytotoxicity assay on Kym-1 cells the results were more in line with expectations, seeing a negative correlation between STAR2 concentration and cell viability. This was primarily the case for the 37°C compound, which showed a clear negative correlation for the group results as well as in both individual plates. For the 4°C compound, the correlation was only clearly visible in the plate containing no clear contamination. Even though this was the case, it was not expected that the 37°C compound would show a better negative correlation than the 4°C stored compound. A possible explanation for this phenomenon could lie in the degradation of the STAR2 compound. It could be that when the compound is stored at 37°C it slowly degrades or oxidizes into toxic breakdown products. The fact that the difference in cell viability between the 4°C and 37°C stored compound is highest at 1000 ng/mL supports the idea that even more cytotoxic breakdown products are being formed when STAR2 is stored at 37°C. By addressing this possibility we also come to one of the flaws of this experiment. Due to STAR2's effectiveness being tested through its cytotoxicity all other cytotoxic pathways of the molecule are also taken into consideration and are thus effectively masked by the experimental setup. Although no published data currently demonstrate that STAR2 produces toxic degradation products when stored at 37°C, it is generally accepted that higher concentrations of biologically active compounds can induce off-target cytotoxic effects (Rang & Dale's Pharmacology, 2023). Additionally, protein-based therapeutics are known to degrade over time at elevated temperatures, which can lead to the formation of bioactive or toxic byproducts (Wang, 1999). To eliminate these effects from the equation, you would have to run an extra control experiment with a different cell line not expressing TNFR1 & TNFR2 receptors and assess the compound's cytotoxicity there as well.

For the behavioral analysis, no significant differences between the two groups could be found; this still applied when the sexes were separated. This insignificance is likely to have occurred due to the Y-maze not being the right behavioral test to address hippocampal damage. The Y-maze is known to evaluate short-term working memory; this is however not primarily hippocampus dependent, allowing other brain regions to take over in the case of damage in the J20 model. "Short-term working memory evaluated in the Y-maze is mediated by neurons in the pre-frontal cortex, ventral striatum and hippocampus, whereas spatial learning memory assessed in the MWM is mainly hippocampus-dependent." (Orti-Casañ et al., 2023). Due to the nature of the Y-maze test, detecting significant differences was difficult, even though hippocampal function could have already been compromised in the J20 model. To have a better look into the hippocampal functioning of the mice a different behavioural test like the morriswatermaze (MWM) should be chosen. Taking all this into

consideration, the results from the Y-maze videos were as expected. Looking into the future, it could be of great interest to not only look at a TNFR1 antagonist but also include a behavioral study for a TNFR2 agonist like STAR2 especially since the cytotoxicity assay also involved STAR2.

This report explored whether TNF(- α) modulation is a viable therapeutic approach to improve working memory in Alzheimer's disease models. While immunostaining data were inconclusive due to technical limitations and poor signal quality, the cytotoxicity assay revealed a dose-dependent STAR2 cytotoxic effect, indicating biological activity of the compound. The behavioral Y-maze analysis revealed no significant improvement in working memory after TNFR1-antagonist treatment, likely due to test limitations rather than treatment inefficacy. Although definitive conclusions could not be made, these findings provide preliminary support for further research into TNFR-targeted therapies.

AI use declaration:

During the writing of this report, OpenAI's ChatGPT was used in a professional manner. The tool was used to improve sentence clarity, enhance overall structure, and provide support with R code development and troubleshooting. All content was reviewed and edited by the author to ensure accuracy and appropriateness.

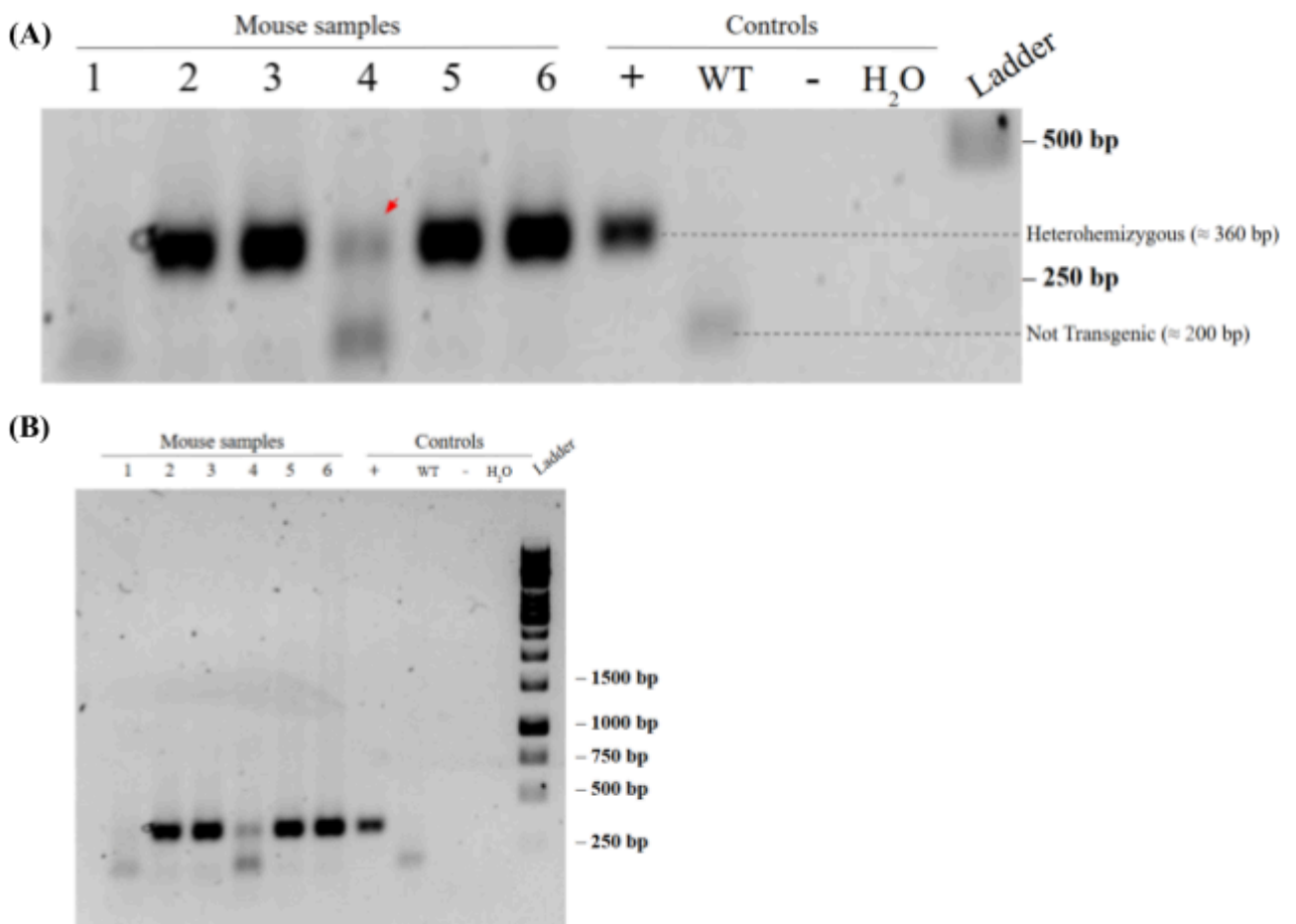
References:

- Bourteele, S., Haußer, A., Döppler, H., Horn-Müller, J., Röpke, C., Schwarzmann, G., Pfizenmaier, K., & Müller, G. (1998). Tumor necrosis factor induces ceramide oscillations and negatively controls sphingolipid synthases by caspases in apoptotic KYM-1 cells. *Journal of Biological Chemistry*, 273(47), 31245–31251. <https://doi.org/10.1074/jbc.273.47.31245>
- Decourt, B., Lahiri, D. K., & Sabbagh, M. N. (2016). Targeting tumor necrosis factor Alpha for Alzheimer's disease. *Current Alzheimer Research*, 14(4), 412–425. <https://doi.org/10.2174/1567205013666160930110551>
- Dong, Y., Dekens, D., De Deyn, P., Naudé, P., & Eisel, U. (2015). Targeting of tumor necrosis factor alpha receptors as a therapeutic strategy for neurodegenerative disorders. *Antibodies*, 4(4), 369–408. <https://doi.org/10.3390/antib4040369>
- Dong, Y., Fischer, R., Naudé, P. J. W., Maier, O., Nyakas, C., Duffey, M., Van Der Zee, E. A., Dekens, D., Douwenga, W., Herrmann, A., Guenzi, E., Kontermann, R. E., Pfizenmaier, K., & Eisel, U. L. M. (2016). Essential protective role of tumor necrosis factor receptor 2 in neurodegeneration. *Proceedings of the National Academy of Sciences*, 113(43), 12304–12309. <https://doi.org/10.1073/pnas.1605195113>
- Fischer, R., Kontermann, R., & Maier, O. (2015). Targeting STNF/TNFR1 signaling as a new therapeutic strategy. *Antibodies*, 4(1), 48–70. <https://doi.org/10.3390/antib4010048>
- Fontaine, V., Mohand-Said, S., Hanoteau, N., Fuchs, C., Pfizenmaier, K., & Eisel, U. (2002). Neurodegenerative and neuroprotective effects of tumor necrosis factor (TNF) in retinal ischemia: opposite roles of TNF receptor 1 and TNF receptor 2. *Journal of Neuroscience*, 22(7), RC216. <https://doi.org/10.1523/jneurosci.22-07-j0001.2002>
- Hampel, H., Vassar, R., De Strooper, B., Hardy, J., Willem, M., Singh, N., Zhou, J., Yan, R., Vanmechelen, E., De Vos, A., Nisticò, R., Corbo, M., Pietro Imbimbo, B., Streffer, J., Voytyuk, I., Timmers, M., Monfared, A. a. T., Irizarry, M., Albalá, B., . . . Vergallo, A. (2020). The B-Secretase BACE1 in Alzheimer's disease. *Biological Psychiatry*, 89(8), 745–756. <https://doi.org/10.1016/j.biopsych.2020.02.001>

- Hong, S., Beja-Glasser, V. F., Nfonoyim, B. M., Frouin, A., Li, S., Ramakrishnan, S., Merry, K. M., Shi, Q., Rosenthal, A., Barres, B. A., Lemere, C. A., Selkoe, D. J., & Stevens, B. (2016). Complement and microglia mediate early synapse loss in Alzheimer mouse models. *Science*, *352*(6286), 712–716. <https://doi.org/10.1126/science.aad8373>
- Jupp, O. J., McFARLANE, S. M., Anderson, H. M., Littlejohn, A. F., Mohamed, A. A., MacKAY, R. H., Vandenabeele, P., & MacEWAN, D. J. (2001). Type II tumour necrosis factor- α receptor (TNFR2) activates c-Jun N-terminal kinase (JNK) but not mitogen-activated protein kinase (MAPK) or p38 MAPK pathways. *Biochemical Journal*, *359*(3), 525. <https://doi.org/10.1042/0264-6021:3590525>
- Karl, T., Bhatia, S., Cheng, D., Kim, W. S., & Garner, B. (2011). Cognitive phenotyping of amyloid precursor protein transgenic J20 mice. *Behavioural Brain Research*, *228*(2), 392–397. <https://doi.org/10.1016/j.bbr.2011.12.021>
- Marchetti, L., Klein, M., Schlett, K., Pfizenmaier, K., & Eisel, U. L. (2004). Tumor Necrosis Factor (TNF)-mediated Neuroprotection against Glutamate-induced Excitotoxicity Is Enhanced by N-Methyl-D-aspartate Receptor Activation. *Journal of Biological Chemistry*, *279*(31), 32869–32881. <https://doi.org/10.1074/jbc.m311766200>
- Naudé, P. J. W., Nyakas, C., Eiden, L. E., Ait-Ali, D., Heide, R., Engelborghs, S., Luiten, P. G. M., De Deyn, P. P., Boer, J. A., & Eisel, U. L. M. (2012). Lipocalin 2: Novel component of proinflammatory signaling in Alzheimer's disease. *The FASEB Journal*, *26*(7), 2811–2823. <https://doi.org/10.1096/fj.11-202457>
- Oddo, S., Caccamo, A., Shepherd, J. D., Murphy, M., Golde, T. E., Kaye, R., Metherate, R., Mattson, M. P., Akbari, Y., & LaFerla, F. M. (2003). Triple-Transgenic Model of Alzheimer's Disease with Plaques and Tangles. *Neuron*, *39*(3), 409–421. [https://doi.org/10.1016/s0896-6273\(03\)00434-3](https://doi.org/10.1016/s0896-6273(03)00434-3)
- Ortí-Casañ, N., Wajant, H., Kuiperij, H. B., Hooijsma, A., Tromp, L., Poortman, I. L., Tadema, N., De Lange, J. H., Verbeek, M. M., De Deyn, P. P., Naudé, P. J., & Eisel, U. L. (2023). Activation of TNF Receptor 2 Improves Synaptic Plasticity and Enhances Amyloid- β Clearance in an Alzheimer's Disease Mouse Model with Humanized TNF Receptor 2. *Journal of Alzheimer S Disease*, *94*(3), 977–991. <https://doi.org/10.3233/jad-221230>
- Ortí-Casañ, N., Wu, Y., Naudé, P. J. W., De Deyn, P. P., Zuhorn, I. S., & Eisel, U. L. M. (2019). Targeting TNFR2 as a novel therapeutic strategy for Alzheimer's disease. *Frontiers in Neuroscience*, *13*. <https://doi.org/10.3389/fnins.2019.00049>
- Ortí-Casañ, N., Zuhorn, I. S., Naudé, P. J. W., De Deyn, P. P., Van Schaik, P. E. M., Wajant, H., & Eisel, U. L. M. (2022). A TNF receptor 2 agonist ameliorates neuropathology and improves cognition in an Alzheimer's disease mouse model. *Proceedings of the National Academy of Sciences*, *119*(37). <https://doi.org/10.1073/pnas.2201137119>
- Prinz, M., Jung, S., & Priller, J. (2019). Microglia Biology: One Century of Evolving Concepts. *Cell*, *179*(2), 292–311. <https://doi.org/10.1016/j.cell.2019.08.053>
- Ramos-Vara, J. A. (2005). Technical aspects of immunohistochemistry. *Veterinary Pathology*, *42*(4), 405–426. <https://doi.org/10.1354/vp.42-4-405>
- Rang & Dale's pharmacology* (10th ed.). (2023). Elsevier - Health Sciences Division.
- Skartsis, N., Ferreira, L. M. R., & Tang, Q. (2022). The dichotomous outcomes of TNF α signaling in CD4+ T cells. *Frontiers in Immunology*, *13*. <https://doi.org/10.3389/fimmu.2022.1042622>
- Steelman, A. J., & Li, J. (2011). Poly(I:C) promotes TNF α /TNFR1-dependent oligodendrocyte death in mixed glial cultures. *Journal of Neuroinflammation*, *8*(1), 89. <https://doi.org/10.1186/1742-2094-8-89>

- Storz, P., Döppler, H., Horn-Müller, J., Müller, G., & Pfizenmaier, K. (2000). TNF down-regulation of receptor tyrosine kinase-dependent mitogenic signal pathways as an important step in cytostasis induction and commitment to apoptosis of Kym-1 rhabdomyosarcoma cells. *Cell Death and Differentiation*, 7(10), 955–965. <https://doi.org/10.1038/sj.cdd.4400732>
- Tosh, J. L., Rickman, M., Rhymes, E., Norona, F. E., Clayton, E., Mucke, L., Isaacs, A. M., Fisher, E. M., & Wiseman, F. K. (2018). The integration site of the APP transgene in the J20 mouse model of Alzheimer’s disease. *Wellcome Open Research*, 2, 84. <https://doi.org/10.12688/wellcomeopenres.12237.2>
- Wang, W. (1999). Instability, stabilization, and formulation of liquid protein pharmaceuticals. *International Journal of Pharmaceutics*, 185(2), 129–188. [https://doi.org/10.1016/s0378-5173\(99\)00152-0](https://doi.org/10.1016/s0378-5173(99)00152-0)
- Wilson, D. M., Cookson, M. R., Van Den Bosch, L., Zetterberg, H., Holtzman, D. M., & Dewachter, I. (2023). Hallmarks of neurodegenerative diseases. *Cell*, 186(4), 693–714. <https://doi.org/10.1016/j.cell.2022.12.032>
- World Health Organization: WHO & World Health Organization: WHO. (2025, March 31). *Dementia*. <https://www.who.int/news-room/fact-sheets/detail/dementia>
- Zhang, J., Zhang, Y., Wang, J., Xia, Y., Zhang, J., & Chen, L. (2024). Recent advances in Alzheimer’s disease: Mechanisms, clinical trials and new drug development strategies. *Signal Transduction and Targeted Therapy*, 9(1). <https://doi.org/10.1038/s41392-024-01911-3>

Supplementary figures:



Supplementary figure 1: (A) gel electrophoresis result after mouse tail DNA isolation red arrow indicates spillover from nearby well (3 or 5) generating faint band, (B) full gel image